Preprints.org

Review

Not peer-reviewed version

An examination of the very first polarimetric X-ray observations of radio-quiet active galactic nuclei

Frédéric Marin * , Vittoria Elvezia Gianolli , Adam Ingram , Dawoon E Kim , Andrea Marinucci , Daniele Tagliacozzo , Francesco Ursini

Posted Date: 17 June 2024

doi: 10.20944/preprints202406.1150.v1

Keywords: X-ray polarization; high-energy processes; black holes

Preprints.org is a free multidiscipline platform providing preprint service that is dedicated to making early versions of research outputs permanently available and citable. Preprints posted at Preprints.org appear in Web of Science, Crossref, Google Scholar, Scilit, Europe PMC.

Copyright: This is an open access article distributed under the Creative Commons Attribution License which permits unrestricted use, distribution, and reproduction in any medium, provided the original work is properly cited.

Preprints.org (www.preprints.org) | NOT PEER-REVIEWED | Posted: 17 June 2024 doi:10.20944/preprints202406.1150.v1

Disclaimer/Publisher's Note: The statements, opinions, and data contained in all publications are solely those of the individual author(s) and contributor(s) and not of MDPI and/or the editor(s). MDPI and/or the editor(s) disclaim responsibility for any injury to people or property resulting from any ideas, methods, instructions, or products referred to in the content.

Review

An Examination of the Very First Polarimetric X-ray Observations of Radio-Quiet Active Galactic Nuclei

Frédéric Marin [1,*], Vittoria E. Gianolli [2,3], Adam Ingram [4], Dawoon E. Kim [5,6,7], Andrea Marinucci [8], Daniele Tagliacozzo [3] and Francesco Ursini [3]

1 Université de Strasbourg, CNRS, Observatoire astronomique de Strasbourg, UMR 7550, F-67000 Strasbourg, France
2 Université Grenoble Alpes, CNRS, IPAG, 38000 Grenoble, France
3 Dipartimento di Matematica e Fisica, Università degli Studi Roma Tre, Via della Vasca Navale 84, 00146 Roma, Italy
4 School of Mathematics, Statistics, and Physics, Newcastle University, Newcastle upon Tyne NE1 7RU, UK
5 INAF Istituto di Astrofisica e Planetologia Spaziali, Via del Fosso del Cavaliere 100, 00133 Roma, Italy
6 Dipartimento di Fisica, Università degli Studi di Roma "La Sapienza", Piazzale Aldo Moro 5, 00185 Roma, Italy
7 Dipartimento di Fisica, Università degli Studi di Roma "Tor Vergata", Via della Ricerca Scientifica 1, 00133 Roma, Italy
8 ASI - Agenzia Spaziale Italiana, Via del Politecnico snc, 00133 Roma, Italy
* Correspondence: frederic.marin@astro.unistra.fr

Abstract: Active galactic nuclei (AGNs), either radio-quiet or radio-loud, had never been observed in X-ray polarized light until the advent of the Imaging X-ray Polarimetry Explorer (IXPE [1]) in the end of 2021. This satellite opened a new observational window for studying supermassive black holes and their complex environment. In this regard, radio-quiet AGNs are probably better targets than radio-loud objects to probe accretion processes, due to the lack of synchrotron emission from jets that can dilute the polarized signal from the central engine. Their relatively clean environment not only allows to detect and measure the X-ray polarization originating from the hot corona responsible for X-ray emission, but also to assess the geometry of the media immediately surrounding the supermassive black hole. Such geometrical measurements work just as well for characterizing the corona morphology in pole-on AGNs as it does for determining the three-dimensional shape of the circumnuclear cold obscurer (the so-called torus) in edge-on AGNs. In this review paper, we will return to each of the observations made by IXPE so far in the field of radio-quiet AGNs and highlight the fundamental contribution of X-ray polarimetry to our understanding of how light is emitted and how matter is shaped around supermassive black holes.

Keywords: X-ray polarization; high-energy processes; black holes

1. Introduction

Observing active galactic nuclei (AGNs) in X-rays is a critical aspect of modern astrophysics, providing insights into some of the universe's most energetic phenomena. AGNs, powered by accretion onto supermassive black holes, emit across the electromagnetic spectrum, but X-ray observations are particularly valuable since, in absence of a jet, such high energy emission comes only from the immediate vicinity of the black hole. The region responsible for it, the X-ray corona, is pictured as a hot, diffuse region close to the potential well, but its size, shape, location and origin remain unclear [2–4].

The most accepted scenario to explain the X-ray emission from coronae is that ultraviolet photons, thermally emitted by the accretion disk, are up-scattered by the electrons in the corona. The resulting X-ray photons we measure are emitted towards the observer or relativistically bent towards the disk surface, where they are reflected back to the observer. The total X-ray spectrum we observe then consists of fluorescence lines, including a prominent $\sim$ 6.4 keV iron Kα line and a broad Compton hump peaking at $\sim$ 20-30 keV, that relativistic effects asymmetrically smear [5]. The scattered photons can be highly polarised whereas the fluorescence lines are unpolarized, making X-ray polarimetric measurements a gold mine for discoveries about emission and diffusion near potential wells.

Probing the corona is feasible if the AGN has a favourable pole-on (type-1) inclination, but in the case of edge-on (type-2) objects, the observer's line-of-sight is intercepted by a thick circumnuclear

© 2024 by the author(s). Distributed under a Creative Commons CC BY license.

Preprints.org (www.preprints.org) | NOT PEER-REVIEWED | Posted: 17 June 2024 doi:10.20944/preprints202406.1150.v1

structure made of dust and gas. In this case, X-rays, with their high penetrating power, interact with these dense regions and allow us to study both the properties of the obscured AGN and the intervening material. This capability is vital for understanding the demographics and evolution of AGNs, as type-2 AGNs constitute a significant portion of the AGN population [6].

By probing the X-ray emissions from AGNs, we can gain deeper insights into the fundamental physical conditions and processes near supermassive black holes. This includes determining the nature of the X-ray corona, exploring the effects of relativistic phenomena, and understanding the composition and behavior of obscuring materials in type-2 AGNs [7]. These studies are pivotal for constructing a comprehensive picture of AGN activity and its impact on the host galaxies and the broader cosmic environment. Great advances were achieved thanks to X-ray spectroscopy and timing analyses [8], but X-ray polarization observations can provide an additional, powerful tool for probing the unknowns of the X-ray corona and the obscuring material in AGNs. Polarization offers a complementary perspective by measuring the orientation and degree of the X-ray emissions' polarization. This can yield crucial information about the geometry and physical conditions of the emitting and scattering regions.

In this review paper, we will examine all the radio-quiet AGNs observed so far thanks to the first X-ray polarimeter sensitive enough to extra-galactic objects. We will demonstrate why polarimetric measurements at high energies are crucial for studying energy transport and radiation processes around supermassive black holes. Section 2 will focus on type-1 AGNs, where the X-ray corona is directly accessible to the observer. Section 3 will summarize the findings about type-2 AGNs, where the central source is obscured by dust and gas. Only Compton-thick sources, i.e. in which the X-ray spectrum is dominated by reflection, will be presented since IXPE did not observe any Compton-thin type-2 AGNs yet. Section 4 will allow us to put the results obtained between 2021 and 2024 in perspective and we will conclude our review in Section 5. Throughout this paper, we define P as the linear polarization degree and Ψ as the electric vector polarization position angle.

2. Type-1 AGNs: Probing the X-ray Corona

Polarization measurements are particularly valuable in constraining the geometry of the X-ray corona. Theoretical models predict that different configurations of the corona – such as slab-like, spherical, or patchy distributions – will produce distinct polarization signatures [9–13]. For example, horizontally extended coronae are expected to show vertical polarization position angles (parallel to the jet position angle, if any), while their polarisation degree are expected to increase with asymmetry (and therefore with viewer inclination). Therefore, by measuring the polarization of X-rays emitted from the corona, we can discern its shape and structure, which is otherwise challenging to determine [14]. This information is critical for understanding how the corona interacts with the accretion disk and contributes to the overall emission profile of the AGN.

Furthermore, X-ray polarization can shed light on the location of the corona relative to the black hole and accretion disk. Variations in polarization with energy (and time) can reveal the location (and the evolution) of the corona, providing (dynamic) insights into how energy is transported and dissipated in the vicinity of the black hole [15,16]. These measurements can help refine models of coronal heating and cooling processes, and the mechanisms by which the corona is maintained.

For those reasons, IXPE was pointed towards three distinct radio-quiet type-1 AGNs during its first two years of operation. We will now briefly describe each observation and the constraints obtained from them.

2.1. MCG-05-23-16

MCG-05-23-16 is a nearby (z=0.0085 [17]), relatively bright ($F_{2-10\ \mathrm{keV}}$=7-10$\times10^{-11}$ erg cm^{-2} s^{-1} [18]) and moderately absorbed ($N_H \sim 10^{22}$ cm^{-2}) Seyfert 1.9 galaxy. In the last decades, extensive observations in the X-rays led to a well determined shape of the primary continuum, with a variable spectral index $\Gamma = 1.75 - 1.85$ and a high energy cut-off $E_C = 100 - 160$ keV [19]. The associated coronal parameters have been also inferred in multiple geometrical configurations with several Comp-

Preprints.org (www.preprints.org) | NOT PEER-REVIEWED | Posted: 17 June 2024 doi:10.20944/preprints202406.1150.v1

tonization models. X-ray polarization, in this context, offers the opportunity of revealing the geometry of the scattering hot corona. Spectral features ascribed to reflection off the accretion disk and distant, cold material are also present in the X-ray spectrum of MCG-05-23-16 and they have been found to be rather stable throughout the years ([20] and references therein). The source was therefore observed by *IXPE* in May and in November 2022 for a total net exposure time of 1.13 Ms, partly simultaneously with *XMM-Newton* and *NuSTAR* to separate and characterize the different spectral features [21,22]).

The analysis of the combined *IXPE*, *XMM-Newton* and *NuSTAR* data confirmed the presence of three spectral components: relativistic ionized reflection from the accretion disk, neutral reflection from distant material and a cutoff power law, which contributes ∼95% of the total 2-8 keV flux. The combined May and November *IXPE* observations provided an upper limit $P = 3.2\%$ to the polarization degree (at 99% of confidence level on one single parameter). The contour plot between the polarization degree P and the polarization angle Ψ is shown in Figure 1 (orange contours). Hints of an alignment between Ψ and the position angle of the [OIII] emission are present ($\sim 40°$, associated to the narrow line region and assumed to be aligned with the accretion disk axis [23]). The comparison between *IXPE* data and numerical simulations obtained with the Monte Carlo code MONK [24] in different geometries led to the inclination angle of the source (i <40°), in good agreement with the one estimated via the modelling of the broad Iron Kα profile ($i = 32°$-$51°$: [20]). Among the several geometrical configurations tested, the conical outflow scenario was ruled out.

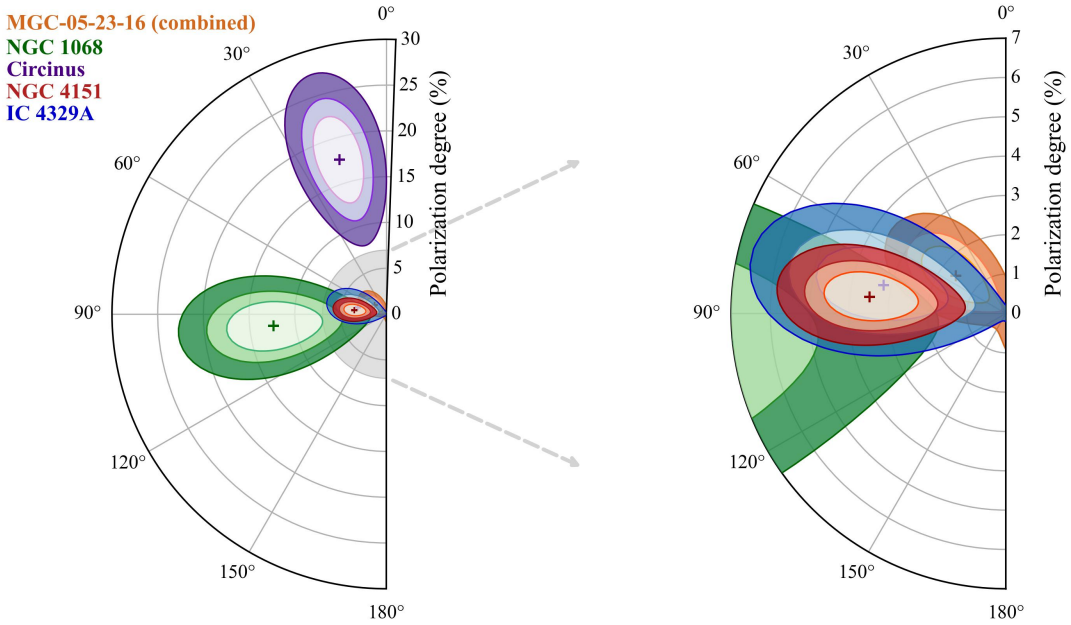

Figure 1. Summary of polarimetric measurements obtained by IXPE in the case of radio-quiet AGNs using contour plots (68-90-99% confidence levels for two degrees of freedom). All spectro-polarimetric fits have been performed using weighted data. The polarization degree and the polarization angle are integrated over the whole 2-8 keV band. The figure on the right is a zoomed-in view of the central region of the left figure for clarity purposes.

2.2. IC 4329A

IC 4329A (redshift $z = 0.0161$, [25]) is a type-1.2 Seyfert galaxy [26]. Its 2–10 keV flux is in the range $F_{2-10\ \mathrm{keV}} \sim (0.1 - 1.8) \times 10^{-10}$ erg s^{-1} cm^{-2} [e.g., 27], making it one of the brightest AGNs in the X-ray sky. The mass of the central black hole is estimated by optical reverberation mapping to be $M \approx 7 \times 10^7 M_\odot$ [28]. The host galaxy appears edge-on, with optical images clearly showing that the dust lane associated with the galaxy's spiral arms cuts across our view of the nucleus [29]. Since the type-1.2 classification implies that we observe the AGN from a rather low inclination, it would indicate that the AGN torus might be misaligned with the galaxy rotation axis.

Preprints.org (www.preprints.org) | NOT PEER-REVIEWED | Posted: 17 June 2024 doi:10.20944/preprints202406.1150.v1

IXPE observed IC 4329A on 2023 January 5–15 for an exposure time of 458 ks [30] (ObsID 01003601). The observation was supported by *XMM-Newton* (January 11–12) and *NuSTAR* (January 11–13) exposures, which indicated that the X-ray continuum had spectral index $\Gamma \approx 1.7$ and electron temperature $kT_e \approx 40$ keV, consistent with earlier observations [27,31]. *IXPE* detected polarization in the 2–8 keV band with 2.97σ confidence (98.78% confidence for two parameters of interest), with polarization degree $P = 3.3\% \pm 1.1\%$ and polarization angle $\Psi = 78^\circ \pm 10^\circ$ (uncertainties are 1σ for a single parameter of interest). The contour plots of P and Ψ are shown in Figure 1 (blue). The polarization angle is consistent with the jet position angle inferred from a September 2021 ALMA observation.

Detailed spectral analysis confirmed the presence of a directly observed coronal component, a relativistic reflector and a distant reflector. The direct continuum contributes $\approx 66\%$ of the 2–8 keV flux, the relativistic reflector contributes $\approx 33\%$, and the distant reflector $\approx 1\%$. A joint *IXPE*/*XMM*/*NuSTAR* spectro-polarimetric analysis indicates that the polarization of the direct continuum component aligns with the overall 2–8 keV polarization, whereas the polarization of the relativistic reflector is unconstrained [30]. It was concluded that the polarization of the corona is consistent with being aligned with the jet, and thus that the corona is most likely extended in the disk plane perpendicular to the jet. Constraints from the relativistic reflector point to a reasonably low viewer inclination ($i < 39^\circ$ with 99% confidence), which is in mild tension with the reasonably high best fitting polarization degree of $P = 3.3 \pm 1.1\%$.

2.3. NGC 4151

NGC 4151 is one of the brightest Seyfert galaxies in the local universe ($z = 0.0033$;[32]), going from optical type 1.5 at high flux states (up to $F_{2-10\,\mathrm{keV}} \sim 3\times 10^{-10}$ erg s^{-1} cm^{-2}) to optical type 1.8 at low fluxes states ($F_{2-10\,\mathrm{keV}} \sim 5\times 10^{-11}$ erg s^{-1} cm^{-2}; see [33,34]). Intensively observed by all major X-ray satellites, the AGN shows significant spectral variability and complex absorption structures (involving combinations of neutral and ionized absorbers of about 10^{22-23} cm^{-2}; e.g., [35–37]). NGC 4151 shows mixed evidence for relativistic reflection off the inner accretion disk (e.g., [36,37]) and a non-relativistic jet (e.g., [38]). Identified as a high priority target for *IXPE* in its first year of operations, it was observed in December 2022 (ObsID 02003101), simultaneously to *NuSTAR* and XMM observations, to constrain the geometry of its hot coronal environment.

From the IXPE observation, NGC 4151 showed $P = 4.9\% \pm 1.1\%$ and $\Psi = 86^\circ \pm 7^\circ$ in the 2-8 keV energy range, corresponding to a $\sim 4.4\sigma$ significance based on a model-independent polarization analysis [37]. Energy-resolved polarization analysis indicated statistically significant polarization variations with energy, showing $P = 4.3\% \pm 1.6\%$ and $\Psi = 42^\circ \pm 11^\circ$ in the 2-3.5 keV soft energy range, differing from measurements in other energy ranges. With a spectro-polarimetric analysis, accounting for polarization dilution in the soft energy regime and setting the polarization angle of the primary emission and reflection emission components as perpendicular, the primary emission component was measured with $P = 7.7\% \pm 1.5\%$ and $\Psi = 87^\circ \pm 6^\circ$. For the reflection component, an upper limit of $P < 27\%$ was derived. The measured polarization angle of the primary component aligns with the direction of NGC 4151's radio jet feature previously obtained by VLBI observations, $\sim 83^\circ$ [39–41]. Therefore, this result disfavors the lamppost and conical geometry scenarios among the proposed coronal geometries and suggest slab or wedge-like geometries. Additionally, the observed polarization angle in the soft energy band is similar to that of the projected angle of the extended narrow-line region (NLR), $45^\circ \pm 5^\circ$, confirmed by HST [42,43] and supported by *Chandra* observations [44], suggesting that a new emission component may influence the X-ray polarization, requiring further observations for confirmation.

Currently, the source has been selected for a second observation during the 1st Cycle of the *IXPE* General Observer program.

Preprints.org (www.preprints.org) | NOT PEER-REVIEWED | Posted: 17 June 2024 doi:10.20944/preprints202406.1150.v1

3. Type-2 AGNs: The Shape of the Equatorial Obscurer

In the context of type-2 AGNs, X-ray polarization is a key diagnostic for investigating the properties of the obscuring material. The polarization of X-rays scattered by the cold component (the dusty torus) or other intervening structures (such as the polar winds – the warm component) can reveal the composition and three-dimensional distribution of these materials. For instance, the scattered X-rays degree of polarization can help to infer the geometry and orientation of the cold component, while variations in polarization across different time bins can map the clumpiness of the obscuring material [45,46]. Those information are vital for understanding the nature of the obscurer and its impact on the observed properties of AGNs.

Moreover, polarization measurements can distinguish between different scattering and absorption processes that occur within the obscuring material. By analyzing the polarization degree and angle, we can infer whether the X-rays are predominantly absorbed by neutral atoms, ionized gas, or dust, and how these components are distributed around the AGN [47]. This can provide insights into the physical and chemical conditions within the obscuring structures, and how they evolve over cosmological time.

Because type-2 AGNs are less bright than type-1s in X-rays, IXPE was only pointed twice towards type-2 objects. We will now briefly describe each observation and the constraints obtained from them.

3.1. The Circinus Galaxy

The Circinus galaxy is the X-ray brightest Compton-thick AGN, and the first one of its class observed by IXPE. The primary X-ray emission of this source is obscured by a large column density, exceeding 6×10^{24} cm^{-2} [48]. The X-ray spectrum in the IXPE energy band is known to be dominated by two emission components: warm reflection off ionized, optically thin matter, and cold reflection off the optically thick torus. Several spectral features are observed, including a strong iron Kα emission line and many other lines from lighter elements [49–51]. Optical and radio observations show the clear presence of [O III] ionization cones [52] and a radio jet [53,54]. Very long baseline interferometry observations of the 1.3-cm water maser emission indicate that the accretion disk is warped and seen edge-on [55].

The Circinus galaxy was observed by IXPE for a net exposure time of 771.5 ks, starting from July 12, 2022 (ObsID 01003501). IXPE measured a 2–6 keV polarization degree P of 20.0% $\pm$ 3.8%, with a polarization angle Ψ of 19.1° $\pm$ 5.5° [56]. The polarization angle is perpendicular to the position angle of the radio jet, and compatible with the direction of the inner water maser disk. In the 6–8 keV band, the polarization is not significantly detected, very likely because of the dilution by the unpolarized fluorescent iron lines. To assess the contribution of the ultraluminous X-ray (ULX) sources in the Circinus field [57], two 10-ks *Chandra* observations were also performed, at the beginning and end of the IXPE exposure (ObsIDs 25365 and 25366). However, the ULXs are definitely subdominant in the IXPE bandpass. The warm reflector gives a relatively low contribution to the flux in the IXPE band, thus its polarization is not well constrained. On the other hand, the spectro-polarimetric fit of IXPE and *Chandra* data indicates that the cold reflector has a polarization degree of 28% $\pm$ 7% [56].

The main conclusion is thus that the cold reflector produces a high polarization, perpendicular to the symmetry axis of the system (here traced by the radio jet). This reflector can be readily identified as the pc-scale torus predicted by Unification Models. With this assumption, dedicated numerical simulations [58,59] show that the torus should have an opening angle of 45°-55° [56]. However, this is not the only possible scenario. For example, the IXPE results can also be explained by Compton scattering off a sub-parsec-scale radiation-driven "fountain" [60]; in this case, the origin of the X-ray polarization would be a dusty outflow inside 0.01 pc [61].

3.2. NGC 1068

NGC 1068 is probably one of the most famous type-2 radio-quiet AGNs. It is both optically bright (V = 11.8 mag in a 4.9″ aperture) and located in the nearby Universe (z = 0.00379), making it an ideal

Preprints.org (www.preprints.org) | NOT PEER-REVIEWED | Posted: 17 June 2024 doi:10.20944/preprints202406.1150.v1

target for AGN observations. NGC 1068 is the first non-jetted AGN in which polarized broad lines were discovered in its polarized optical flux spectrum, paving the way for the unified scheme of AGNs and the understanding that, at least at the zeroth-order, type-1 and type-2 AGNs are similar: most of their apparent observational properties can be explained by an orientation effect [62].

NGC 1068 is a Compton-thick type-2 Seyfert galaxy, similarly to the Circinus galaxy, so high polarization degrees were expected from reprocessing onto the cold and/or warm components based on optical/ultraviolet data [47]. To probe the dense environment around the core of NGC 1068, IXPE was pointed towards this target for a net exposure time of 1.15 Ms between January 3 to January 29, 2024 (ObsID 02008001). The satellite measured a 2 – 8 keV polarization degree of $P = 12.4\% \pm 3.6\%$ at an angle of $\Psi = 100.7^\circ \pm 8.3^\circ$ [63]. The observed X-ray polarization angle is found to be perpendicular to the radio structure axis, as in the optical band, implying that the observed X-ray polarization arises from scattering onto material that is preferentially situated well above the equatorial plane.

In addition to the polarimetric observation, two $\sim$ 10 ks *Chandra* snapshots were acquired at the beginning and at the end of the IXPE pointings, on January 4, 2024 (ObsID 29071) and on January 28, 2024 (ObsID 29072), with the Chandra's Advanced CCD Imaging Spectrometer. Thanks to the Chandra data, the contribution of the ULXs could be accounted for in a joint IXPE+Chandra spectral analysis. Unfortunately, the IXPE observation had not enough counts/statistics to remove the degeneracy among the polarization parameters of the warm and cold reflectors in the spectral decomposition, so a torus inclination and half-opening angle could not be immediately deduced. Building on the hypothesis that the warm component polarization is quantitatively similar to the polarization observed in the far-ultraviolet [47,64] and that electron scattering dominates in the wind [64], a putative value for the intrinsic polarization of the cold component could be estimated. From such value, numerical simulations predicts a probable torus half-opening angle of 50 – 55° (from the vertical axis of the system). Interestingly, this range of torus half-opening angles is quite similar to the one derived for the Circinus galaxy (see Section 3.1).

4. Discussion

The first two years of IXPE operation provided us with revolutionary results. In the field of radio-quiet AGNs, five different sources have been observed, with MCG-05-23-16 observed twice. Three were type-1 AGNs, two were type-2s. Figures 1 and 2 show the observed X-ray polarization (in degree and angle) and the required IXPE observing time as a function of the source total flux, respectively. One can see that the 68% confidence contours are quite large despite the hundreds of kiloseconds obtained per target. This highlights the fact that X-ray polarimetry of radio-quiet AGNs is challenging, but rewarding.

Preprints.org (www.preprints.org) | NOT PEER-REVIEWED | Posted: 17 June 2024 doi:10.20944/preprints202406.1150.v1

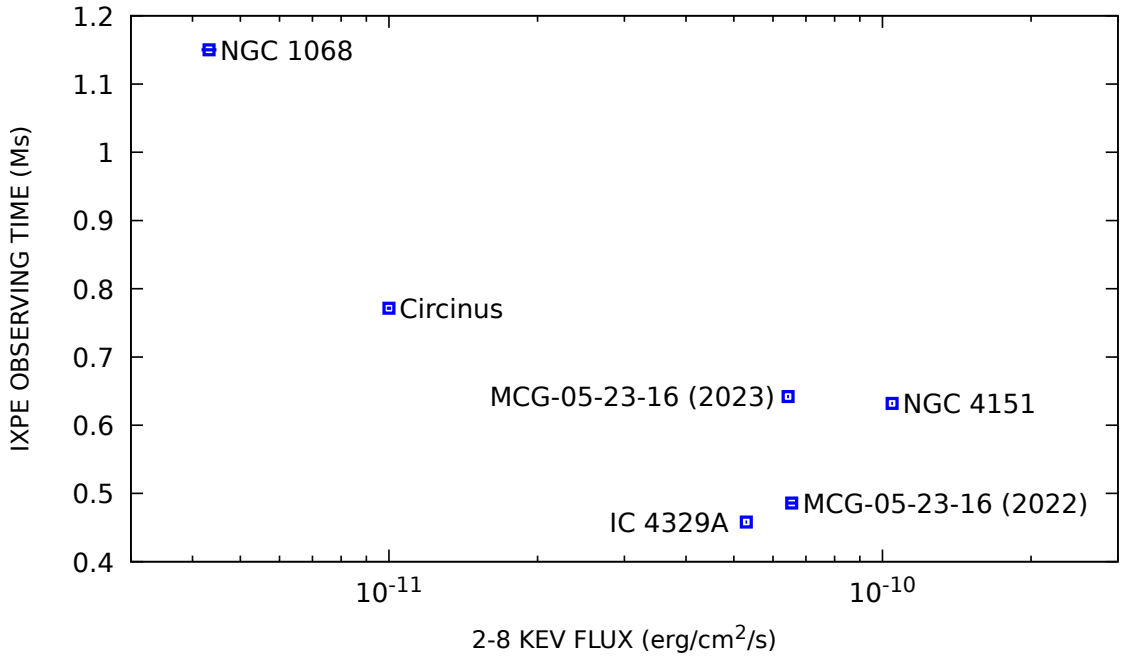

Figure 2. IXPE observing time as a function of the source total flux (in the 2 - 8 keV band). Each target has been labeled.

In the case of type-1 AGNs, if only one solid detection could have been obtained in the case of NGC 4151, it provided an indisputable evidence that the X-ray corona is lying along the equatorial plane. The results obtained for the two other sources, while with less confidence, point towards the same direction. Results obtained in the case of X-ray binaries in the hard state also corroborate this geometrical setup [65]. This has a profound impact on our conception of the high energy generation mechanism around black holes, since an equatorial corona can sandwich the accretion disk, like an atmosphere, or can be located beyond the truncation of the internal radius of the accretion disk. Those geometrical configurations will produce different time-lags than in the case of a lamppost corona, leading to new simulations and interpretations of the temporal variation of the X-ray continuum and fluorescence emission in AGNs.

Results obtained in the case of type-2 Seyfert galaxies also point towards a shared conclusion: the half-opening angle of the cold obscurer is probably around $45 - 55^\circ$ from the vertical axis of the system, at least in those two systems. This is very different to what has been inferred from radio and infrared studies, where the equatorial obscurer is found to be rather geometrically thin [66–68]. This discrepancy is yet to be explained thanks to deeper Circinus and NGC 1068 IXPE observations, as well as X-ray polarimetry of new type-2 targets.

5. Conclusions

X-ray polarization observations offer a unique and powerful means to unravel the complexities of the X-ray corona and the obscuring material in AGNs. By providing detailed information on the geometry, location, and composition of these regions, polarization studies enhance our understanding of the central engines of AGNs and their environments. This, in turn, contributes to a more comprehensive picture of AGNs activity and their role in the evolution of galaxies and the universe.

Author Contributions: Writing—original draft preparation, F.M.; writing—review and editing, V.E.G, A.I., D.E.K., A.M., D.T, F.U.. All authors have read and agreed to the published version of the manuscript.

Funding: The Imaging X-ray Polarimetry Explorer (IXPE) is a joint US and Italian mission. The US contribution is supported by the National Aeronautics and Space Administration (NASA) and led and managed by its Marshall Space Flight Center (MSFC), with industry partner Ball Aerospace (contract NNM15AA18C). The

Preprints.org (www.preprints.org) | NOT PEER-REVIEWED | Posted: 17 June 2024 doi:10.20944/preprints202406.1150.v1

Italian contribution is supported by the Italian Space Agency (Agenzia Spaziale Italiana, ASI) through contract ASI-OHBI-2022-13-I.0, agreements ASI-INAF-2022-19-HH.0 and ASI-INFN-2017.13-H0, and its Space Science Data Center (SSDC) with agreements ASI-INAF-2022-14-HH.0 and ASI-INFN 2021-43-HH.0, and by the Istituto Nazionale di Astrofisica (INAF) and the Istituto Nazionale di Fisica Nucleare (INFN) in Italy. This research used data products provided by the IXPE Team (MSFC, SSDC, INAF, and INFN) and distributed with additional software tools by the High-Energy Astrophysics Science Archive Research Center (HEASARC), at NASA Goddard Space Flight Center (GSFC).

Institutional Review Board Statement: Not applicable

Informed Consent Statement: Not applicable

Data Availability Statement: IXPE observation are public and can be freely downloaded and reduced here : https://heasarc.gsfc.nasa.gov/docs/ixpe/archive/.

Acknowledgments: FM would like to acknowledge the support of the CNRS, the University of Strasbourg, the PNHE and PNCG. This work was supported by the "Programme National des Hautes Énergies" (PNHE) and the "Programme National de Cosmologie et Galaxies (PNCG)" of CNRS/INSU co-funded by CNRS/IN2P3, CNRS/INP, CEA and CNES.

Conflicts of Interest: The authors declare no conflicts of interest.

References

1. Weisskopf, M.C.; Soffitta, P.; Baldini, L.; Ramsey, B.D.; O'Dell, S.L.; Romani, R.W.; Matt, G.; Deininger, W.D.; Baumgartner, W.H.; Bellazzini, R.; Costa, E.; Kolodziejczak, J.J.; Latronico, L.; Marshall, H.L.; Muleri, F.; Bongiorno, S.D.; Tennant, A.; Bucciantini, N.; Dovciak, M.; Marin, F.; Marscher, A.; Poutanen, J.; Slane, P.; Turolla, R.; Kalinowski, W.; Di Marco, A.; Fabiani, S.; Minuti, M.; La Monaca, F.; Pinchera, M.; Rankin, J.; Sgro', C.; Trois, A.; Xie, F.; Alexander, C.; Allen, D.Z.; Amici, F.; Andersen, J.; Antonelli, A.; Antoniak, S.; Attinà, P.; Barbanera, M.; Bachetti, M.; Baggett, R.M.; Bladt, J.; Brez, A.; Bonino, R.; Boree, C.; Borotto, F.; Breeding, S.; Brienza, D.; Bygott, H.K.; Caporale, C.; Cardelli, C.; Carpentiero, R.; Castellano, S.; Castronuovo, M.; Cavalli, L.; Cavazzuti, E.; Ceccanti, M.; Centrone, M.; Citraro, S.; D'Amico, F.; D'Alba, E.; Di Gesu, L.; Del Monte, E.; Dietz, K.L.; Di Lalla, N.; Persio, G.D.; Dolan, D.; Donnarumma, I.; Evangelista, Y.; Ferrant, K.; Ferrazzoli, R.; Ferrie, M.; Footdale, J.; Forsyth, B.; Foster, M.; Garelick, B.; Gunji, S.; Gurnee, E.; Head, M.; Hibbard, G.; Johnson, S.; Kelly, E.; Kilaru, K.; Lefevre, C.; Roy, S.L.; Loffredo, P.; Lorenzi, P.; Lucchesi, L.; Maddox, T.; Magazzu, G.; Maldera, S.; Manfreda, A.; Mangraviti, E.; Marengo, M.; Marrocchesi, A.; Massaro, F.; Mauger, D.; McCracken, J.; McEachen, M.; Mize, R.; Mereu, P.; Mitchell, S.; Mitsuishi, I.; Morbidini, A.; Mosti, F.; Nasimi, H.; Negri, B.; Negro, M.; Nguyen, T.; Nitschke, I.; Nuti, A.; Onizuka, M.; Oppedisano, C.; Orsini, L.; Osborne, D.; Pacheco, R.; Paggi, A.; Painter, W.; Pavelitz, S.D.; Pentz, C.; Piazzolla, R.; Perri, M.; Pesce-Rollins, M.; Peterson, C.; Pilia, M.; Profeti, A.; Puccetti, S.; Ranganathan, J.; Ratheesh, A.; Reedy, L.; Root, N.; Rubini, A.; Ruswick, S.; Sanchez, J.; Sarra, P.; Santoli, F.; Scalise, E.; Sciortino, A.; Schroeder, C.; Seek, T.; Sosdian, K.; Spandre, G.; Speegle, C.O.; Tamagawa, T.; Tardiola, M.; Tobia, A.; Thomas, N.E.; Valerie, R.; Vimercati, M.; Walden, A.L.; Weddendorf, B.; Wedmore, J.; Welch, D.; Zanetti, D.; Zanetti, F. The Imaging X-Ray Polarimetry Explorer (IXPE): Pre-Launch. *Journal of Astronomical Telescopes, Instruments, and Systems* **2022**, *8*, 026002, [arXiv:astro-ph.IM/2112.01269]. doi:10.1117/1.JATIS.8.2.026002.
2. Matt, G.; Perola, G.C.; Piro, L. The iron line and high energy bump as X-ray signatures of cold matter in Seyfert 1 galaxies. *A&A* **1991**, *247*, 25.
3. Middei, R.; Bianchi, S.; Marinucci, A.; Matt, G.; Petrucci, P.O.; Tamborra, F.; Tortosa, A. Relations between phenomenological and physical parameters in the hot coronae of AGNs computed with the MoCA code. *A&A* **2019**, *630*, A131, [arXiv:astro-ph.HE/1908.10373]. doi:10.1051/0004-6361/201935881.
4. Ursini, F.; Matt, G.; Bianchi, S.; Marinucci, A.; Dovčiak, M.; Zhang, W. Prospects for differentiating extended coronal geometries in AGNs with the IXPE mission. *MNRAS* **2022**, *510*, 3674–3687, [arXiv:astro-ph.HE/2112.11268]. doi:10.1093/mnras/stab3745.
5. Matt, G. X-ray Emission and Reprocessing in AGNs. The Central Engine of Active Galactic Nuclei; Ho, L.C.; Wang, J.W., Eds., 2007, Vol. 373, *Astronomical Society of the Pacific Conference Series*, p. 125.
6. Bianchi, S.; Maiolino, R.; Risaliti, G. AGN Obscuration and the Unified Model. *Advances in Astronomy* **2012**, *2012*, 782030, [arXiv:astro-ph.GA/1201.2119]. doi:10.1155/2012/782030.

Preprints.org (www.preprints.org) | NOT PEER-REVIEWED | Posted: 17 June 2024 doi:10.20944/preprints202406.1150.v1

7. Turner, T.J.; Miller, L. X-ray absorption and reflection in active galactic nuclei. *aapr* **2009**, *17*, 47–104, [arXiv:astro-ph.HE/0902.0651]. doi:10.1007/s00159-009-0017-1.
8. Gallo, L.C.; Miller, J.M.; Costantini, E. Active galactic nuclei with high-resolution X-ray spectroscopy. *arXiv e-prints* **2023**, p. arXiv:2302.10930, [arXiv:astro-ph.HE/2302.10930]. doi:10.48550/arXiv.2302.10930.
9. Haardt, F.; Maraschi, L. A Two-Phase Model for the X-Ray Emission from Seyfert Galaxies. *ApJ* **1991**, *380*, L51. doi:10.1086/186171.
10. Henri, G.; Petrucci, P.O. Anisotropic illumination of AGN's accretion disk by a non thermal source. I. General theory and application to the Newtonian geometry. *aap* **1997**, *326*, 87–98, [arXiv:astro-ph/astro-ph/9705233]. doi:10.48550/arXiv.astro-ph/9705233.
11. Ghisellini, G..; Haardt, F.; Matt, G.. Aborted jets and the X-ray emission of radio-quiet AGNs. *A&A* **2004**, *413*, 535–545. doi:10.1051/0004-6361:20031562.
12. Schnittman, J.D.; Krolik, J.H. X-RAY POLARIZATION FROM ACCRETING BLACK HOLES: CORONAL EMISSION. *apj* **2010**, *712*, 908. doi:10.1088/0004-637X/712/2/908.
13. Beloborodov, A.M. Radiative Magnetic Reconnection Near Accreting Black Holes. *ApJ* **2017**, *850*, 141, [arXiv:astro-ph.HE/1701.02847]. doi:10.3847/1538-4357/aa8f4f.
14. Matt, G. X-ray polarization properties of a centrally illuminated accretion disc. *mnras* **1993**, *260*, 663–674. doi:10.1093/mnras/260.3.663.
15. Marin, F.; Goosmann, R.W.; Petrucci, P.O. X-ray polarimetric signatures induced by spectral variability in the framework of the receding torus model. *aap* **2016**, *591*, A23, [arXiv:astro-ph.HE/1604.07562]. doi:10.1051/0004-6361/201628458.
16. Beheshtipour, B.; Krawczynski, H.; Malzac, J. The X-Ray Polarization of the Accretion Disk Coronae of Active Galactic Nuclei. *apj* **2017**, *850*, 14, [arXiv:astro-ph.HE/1710.00247]. doi:10.3847/1538-4357/aa906a.
17. Wegner, G.; Bernardi, M.; Willmer, C.N.A.; da Costa, L.N.; Alonso, M.V.; Pellegrini, P.S.; Maia, M.A.G.; Chaves, O.L.; Rité, C. Redshift-Distance Survey of Early-Type Galaxies: Spectroscopic Data. *aj* **2003**, *126*, 2268–2280, [arXiv:astro-ph/astro-ph/0308357]. doi:10.1086/378959.
18. Mattson, B.J.; Weaver, K.A. RXTE and BeppoSAX Observations of MCG –5-23-16: Reflection from Distant Cold Material. *The Astrophysical Journal* **2004**, *601*, 771. doi:10.1086/380502.
19. Zoghbi, A.; Matt, G.; Miller, J.M.; Lohfink, A.M.; Walton, D.J.; Ballantyne, D.R.; García, J.A.; Stern, D.; Koss, M.J.; Farrah, D.; Harrison, F.A.; Boggs, S.E.; Christensen, F.E.; Craig, W.; Hailey, C.J.; Zhang, W.W. A Long Look at MCG-5-23-16 with NuSTAR. I. Relativistic Reflection and Coronal Properties. *apj* **2017**, *836*, 2, [arXiv:astro-ph.HE/1701.02309]. doi:10.3847/1538-4357/aa582c.
20. Serafinelli, R.; Marinucci, A.; De Rosa, A.; Bianchi, S.; Middei, R.; Matt, G.; Reeves, J.N.; Braito, V.; Tombesi, F.; Gianolli, V.E.; Ingram, A.; Marin, F.; Petrucci, P.O.; Tagliacozzo, D.; Ursini, F. A remarkably stable accretion disc in the Seyfert galaxy MCG-5-23-16. *mnras* **2023**, *526*, 3540–3547, [arXiv:astro-ph.HE/2309.06092]. doi:10.1093/mnras/stad2801.
21. Marinucci, A.; Muleri, F.; Dovciak, M.; Bianchi, S.; Marin, F.; Matt, G.; Ursini, F.; Middei, R.; Marshall, H.L.; Baldini, L.; Barnouin, T.; Rodriguez, N.C.; De Rosa, A.; Di Gesu, L.; Harper, D.; Ingram, A.; Karas, V.; Krawczynski, H.; Madejski, G.; Panagiotou, C.; Petrucci, P.O.; Podgorny, J.; Puccetti, S.; Tombesi, F.; Veledina, A.; Zhang, W.; Agudo, I.; Antonelli, L.A.; Bachetti, M.; Baumgartner, W.H.; Bellazzini, R.; Bongiorno, S.D.; Bonino, R.; Brez, A.; Bucciantini, N.; Capitanio, F.; Castellano, S.; Cavazzuti, E.; Ciprini, S.; Costa, E.; Del Monte, E.; Di Lalla, N.; Di Marco, A.; Donnarumma, I.; Doroshenko, V.; Ehlert, S.R.; Enoto, T.; Evangelista, Y.; Fabiani, S.; Ferrazzoli, R.; Garcia, J.A.; Gunji, S.; Hayashida, K.; Heyl, J.; Iwakiri, W.; Jorstad, S.G.; Kitaguchi, T.; Kolodziejczak, J.J.; La Monaca, F.; Latronico, L.; Liodakis, I.; Maldera, S.; Manfreda, A.; Marscher, A.P.; Mitsuishi, I.; Mizuno, T.; Ng, C.Y.; O'Dell, S.L.; Omodei, N.; Oppedisano, C.; Papitto, A.; Pavlov, G.G.; Peirson, A.L.; Perri, M.; Pesce-Rollins, M.; Pilia, M.; Possenti, A.; Poutanen, J.; Ramsey, B.D.; Rankin, J.; Ratheesh, A.; Romani, R.W.; Sgrš, C.; Slane, P.; Soffitta, P.; Spandre, G.; Tamagawa, T.; Tavecchio, F.; Taverna, R.; Tawara, Y.; Tennant, A.F.; Thomas, N.E.; Trois, A.; Tsygankov, S.S.; Turolla, R.; Vink, J.; Weisskopf, M.C.; Wu, K.; Xie, F.; Zane, S. Polarization constraints on the X-ray corona in Seyfert Galaxies: MCG-05-23-16. *mnras* **2022**, *516*, 5907–5913, [arXiv:astro-ph.HE/2207.09338]. doi:10.1093/mnras/stac2634.
22. Tagliacozzo, D.; Marinucci, A.; Ursini, F.; Matt, G.; Bianchi, S.; Baldini, L.; Barnouin, T.; Cavero Rodriguez, N.; De Rosa, A.; Di Gesu, L.; Dovčiak, M.; Harper, D.; Ingram, A.; Karas, V.; Kim, D.E.; Krawczynski, H.; Madejski, G.; Marin, F.; Middei, R.; Marshall, H.L.; Muleri, F.; Panagiotou, C.; Petrucci, P.O.; Podgorny, J.; Poutanen, J.; Puccetti, S.; Soffitta, P.; Tombesi, F.; Veledina, A.; Zhang, W.; Agudo, I.; Antonelli, L.A.;

Preprints.org (www.preprints.org) | NOT PEER-REVIEWED | Posted: 17 June 2024 doi:10.20944/preprints202406.1150.v1

Bachetti, M.; Baumgartner, W.H.; Bellazzini, R.; Bongiorno, S.D.; Bonino, R.; Brez, A.; Bucciantini, N.; Capitanio, F.; Castellano, S.; Cavazzuti, E.; Chen, C.T.; Ciprini, S.; Costa, E.; Del Monte, E.; Di Lalla, N.; Di Marco, A.; Donnarumma, I.; Doroshenko, V.; Ehlert, S.R.; Enoto, T.; Evangelista, Y.; Fabiani, S.; Ferrazzoli, R.; Garcia, J.A.; Gunji, S.; Heyl, J.; Iwakiri, W.; Jorstad, S.G.; Kaaret, P.; Kislat, F.; Kitaguchi, T.; Kolodziejczak, J.J.; La Monaca, F.; Latronico, L.; Liodakis, I.; Maldera, S.; Manfreda, A.; Marscher, A.P.; Massaro, F.; Mitsuishi, I.; Mizuno, T.; Negro, M.; Ng, C.Y.; O'Dell, S.L.; Omodei, N.; Oppedisano, C.; Papitto, A.; Pavlov, G.G.; Peirson, A.L.; Perri, M.; Pesce-Rollins, M.; Pilia, M.; Possenti, A.; Ramsey, B.D.; Rankin, J.; Ratheesh, A.; Roberts, O.J.; Romani, R.W.; Sgrò, C.; Slane, P.; Spandre, G.; Swartz, D.A.; Tamagawa, T.; Tavecchio, F.; Taverna, R.; Tawara, Y.; Tennant, A.F.; Thomas, N.E.; Trois, A.; Tsygankov, S.S.; Turolla, R.; Vink, J.; Weisskopf, M.C.; Wu, K.; Xie, F.; Zane, S. The geometry of the hot corona in MCG-05-23-16 constrained by X-ray polarimetry. *mnras* **2023**, *525*, 4735–4743, [arXiv:astro-ph.HE/2305.10213]. doi:10.1093/mnras/stad2627.

23. Ferruit, P.; Wilson, A.S.; Mulchaey, J. Hubble Space Telescope WFPC2 Imaging of a Sample of Early-Type Seyfert Galaxies*. *The Astrophysical Journal Supplement Series* **2000**, *128*, 139. doi:10.1086/313379.
24. Wang, J.; Fabbiano, G.; Elvis, M.; Risaliti, G.; Karovska, M.; Zezas, A.; Mundell, C.G.; Dumas, G.; Schinnerer, E. A Deep Chandra ACIS Study of NGC 4151. III. The Line Emission and Spectral Analysis of the Ionization Cone. *apj* **2011**, *742*, 23, [arXiv:astro-ph.CO/1103.1913]. doi:10.1088/0004-637X/742/1/23.
25. Willmer, C.N.A.; Focardi, P.; Chan, R.; Pellegrini, P.S.; da Costa, N.L. Studies of Nearby Poor Clusters: A3574 and S753. *aj* **1991**, *101*, 57. doi:10.1086/115665.
26. Véron-Cetty, M.P.; Véron, P. A catalogue of quasars and active nuclei: 12th edition. *aap* **2006**, *455*, 773–777. doi:10.1051/0004-6361:20065177.
27. Brenneman, L.W.; Madejski, G.; Fuerst, F.; Matt, G.; Elvis, M.; Harrison, F.A.; Ballantyne, D.R.; Boggs, S.E.; Christensen, F.E.; Craig, W.W.; Fabian, A.C.; Grefenstette, B.W.; Hailey, C.J.; Madsen, K.K.; Marinucci, A.; Rivers, E.; Stern, D.; Walton, D.J.; Zhang, W.W. Measuring the Coronal Properties of IC 4329A with NuSTAR. *apj* **2014**, *781*, 83, [arXiv:astro-ph.HE/1312.3563]. doi:10.1088/0004-637X/781/2/83.
28. Bentz, M.C.; Onken, C.A.; Street, R.; Valluri, M. Reverberation Mapping of IC 4329A. *apj* **2023**, *944*, 29, [arXiv:astro-ph.GA/2212.05954]. doi:10.3847/1538-4357/acab62.
29. Mehdipour, M.; Costantini, E. Probing the nature and origin of dust in the reddened quasar IC 4329A with global modelling from X-ray to infrared. *aap* **2018**, *619*, A20, [arXiv:astro-ph.HE/1808.04628]. doi:10.1051/0004-6361/201833706.
30. Ingram, A.; Ewing, M.; Marinucci, A.; Tagliacozzo, D.; Rosario, D.J.; Veledina, A.; Kim, D.E.; Marin, F.; Bianchi, S.; Poutanen, J.; Matt, G.; Marshall, H.L.; Ursini, F.; De Rosa, A.; Petrucci, P.O.; Madejski, G.; Barnouin, T.; Gesu, L.D.; Dovčiak, M.; Gianolli, V.E.; Krawczynski, H.; Loktev, V.; Middei, R.; Podgorny, J.; Puccetti, S.; Ratheesh, A.; Soffitta, P.; Tombesi, F.; Ehlert, S.R.; Massaro, F.; Agudo, I.; Antonelli, L.A.; Bachetti, M.; Baldini, L.; Baumgartner, W.H.; Bellazzini, R.; Bongiorno, S.D.; Bonino, R.; Brez, A.; Bucciantini, N.; Capitanio, F.; Castellano, S.; Cavazzuti, E.; Chen, C.T.; Ciprini, S.; Costa, E.; Del Monte, E.; Lalla, N.D.; Marco, A.D.; Donnarumma, I.; Doroshenko, V.; Enoto, T.; Evangelista, Y.; Fabiani, S.; Ferrazzoli, R.; García, J.A.; Gunji, S.; Heyl, J.; Iwakiri, W.; Jorstad, S.G.; Kaaret, P.; Karas, V.; Kislat, F.; Kitaguchi, T.; Kolodziejczak, J.J.; Monaca, F.L.; Latronico, L.; Liodakis, I.; Maldera, S.; Manfreda, A.; Marscher, A.P.; Mitsuishi, I.; Mizuno, T.; Muleri, F.; Negro, M.; Ng, C.Y.; O'Dell, S.L.; Omodei, N.; Oppedisano, C.; Papitto, A.; Pavlov, G.G.; Peirson, A.L.; Perri, M.; Pesce-Rollins, M.; Pilia, M.; Possenti, A.; Ramsey, B.D.; Rankin, J.; Roberts, O.J.; Romani, R.W.; Sgrò, C.; Slane, P.; Spandre, G.; Swartz, D.A.; Tamagawa, T.; Tavecchio, F.; Taverna, R.; Tawara, Y.; Tennant, A.F.; Thomas, N.E.; Trois, A.; Tsygankov, S.S.; Turolla, R.; Vink, J.; Weisskopf, M.C.; Wu, K.; Xie, F.; Zane, S. The X-ray polarization of the Seyfert 1 galaxy IC 4329A. *mnras* **2023**, *525*, 5437–5449, [arXiv:astro-ph.HE/2305.13028]. doi:10.1093/mnras/stad2625.
31. Brenneman, L.W.; Madejski, G.; Fuerst, F.; Matt, G.; Elvis, M.; Harrison, F.A.; Ballantyne, D.R.; Boggs, S.E.; Christensen, F.E.; Craig, W.W.; Fabian, A.C.; Grefenstette, B.W.; Hailey, C.J.; Madsen, K.K.; Marinucci, A.; Rivers, E.; Stern, D.; Walton, D.J.; Zhang, W.W. The Broad-band X-Ray Spectrum of IC 4329A from a Joint NuSTAR/Suzaku Observation. *apj* **2014**, *788*, 61, [arXiv:astro-ph.HE/1404.7486]. doi:10.1088/0004-637X/788/1/61.
32. Wolfinger, K.; Kilborn, V.A.; Koribalski, B.S.; Minchin, R.F.; Boyce, P.J.; Disney, M.J.; Lang, R.H.; Jordan, C.A. A blind HI survey in the Ursa Major region. *mnras* **2013**, *428*, 1790–1817, [arXiv:astro-ph.CO/1210.2727]. doi:10.1093/mnras/sts160.

Preprints.org (www.preprints.org) | NOT PEER-REVIEWED | Posted: 17 June 2024 doi:10.20944/preprints202406.1150.v1

33. Antonucci, R.R.J.; Cohen, R.D. Time development of the emission lines and continuum of NGC 4151. *apj* **1983**, *271*, 564–574. doi:10.1086/161223.
34. Beuchert, T.; Markowitz, A.G.; Dauser, T.; García, J.A.; Keck, M.L.; Wilms, J.; Kadler, M.; Brenneman, L.W.; Zdziarski, A.A. A Suzaku, NuSTAR, and XMM-Newton view on variable absorption and relativistic reflection in NGC 4151. *aap* **2017**, *603*, A50, [arXiv:astro-ph.HE/1703.10856]. doi:10.1051/0004-6361/201630293.
35. Holt, S.S.; Mushotzky, R.F.; Becker, R.H.; Boldt, E.A.; Serlemitsos, P.J.; Szymkowiak, A.E.; White, N.E. X-ray spectral constraints on the broad-line cloud geometry of NGC 4151. *apjl* **1980**, *241*, L13–L17. doi:10.1086/183350.
36. Keck, M.L.; Brenneman, L.W.; Ballantyne, D.R.; Bauer, F.; Boggs, S.E.; Christensen, F.E.; Craig, W.W.; Dauser, T.; Elvis, M.; Fabian, A.C.; Fuerst, F.; García, J.; Grefenstette, B.W.; Hailey, C.J.; Harrison, F.A.; Madejski, G.; Marinucci, A.; Matt, G.; Reynolds, C.S.; Stern, D.; Walton, D.J.; Zoghbi, A. NuSTAR and Suzaku X-ray Spectroscopy of NGC 4151: Evidence for Reflection from the Inner Accretion Disk. *apj* **2015**, *806*, 149, [arXiv:astro-ph.HE/1504.07950]. doi:10.1088/0004-637X/806/2/149.
37. Gianolli, V.E.; Kim, D.E.; Bianchi, S.; Agís-González, B.; Madejski, G.; Marin, F.; Marinucci, A.; Matt, G.; Middei, R.; Petrucci, P.O.; Soffitta, P.; Tagliacozzo, D.; Tombesi, F.; Ursini, F.; Barnouin, T.; De Rosa, A.; Di Gesu, L.; Ingram, A.; Loktev, V.; Panagiotou, C.; Podgorny, J.; Poutanen, J.; Puccetti, S.; Ratheesh, A.; Veledina, A.; Zhang, W.; Agudo, I.; Antonelli, L.A.; Bachetti, M.; Baldini, L.; Baumgartner, W.H.; Bellazzini, R.; Bongiorno, S.D.; Bonino, R.; Brez, A.; Bucciantini, N.; Capitanio, F.; Castellano, S.; Cavazzuti, E.; Chen, C.T.; Ciprini, S.; Costa, E.; Del Monte, E.; Di Lalla, N.; Di Marco, A.; Donnarumma, I.; Doroshenko, V.; Dovčiak, M.; Ehlert, S.R.; Enoto, T.; Evangelista, Y.; Fabiani, S.; Ferrazzoli, R.; García, J.A.; Gunji, S.; Heyl, J.; Iwakiri, W.; Jorstad, S.G.; Kaaret, P.; Karas, V.; Kislat, F.; Kitaguchi, T.; Kolodziejczak, J.J.; Krawczynski, H.; La Monaca, F.; Latronico, L.; Liodakis, I.; Maldera, S.; Manfreda, A.; Marscher, A.P.; Marshall, H.L.; Massaro, F.; Mitsuishi, I.; Mizuno, T.; Muleri, F.; Negro, M.; Ng, C.Y.; O'Dell, S.L.; Omodei, N.; Oppedisano, C.; Papitto, A.; Pavlov, G.G.; Peirson, A.L.; Perri, M.; Pesce-Rollins, M.; Pilia, M.; Possenti, A.; Ramsey, B.D.; Rankin, J.; Roberts, O.J.; Romani, R.W.; Sgrò, C.; Slane, P.; Spandre, G.; Swartz, D.A.; Tamagawa, T.; Tavecchio, F.; Taverna, R.; Tawara, Y.; Tennant, A.F.; Thomas, N.E.; Trois, A.; Tsygankov, S.S.; Turolla, R.; Vink, J.; Weisskopf, M.C.; Wu, K.; Xie, F.; Zane, S. Uncovering the geometry of the hot X-ray corona in the Seyfert galaxy NGC 4151 with IXPE. *mnras* **2023**, *523*, 4468–4476, [arXiv:astro-ph.GA/2303.12541]. doi:10.1093/mnras/stad1697.
38. Ulvestad, J.S.; Wong, D.S.; Taylor, G.B.; Gallimore, J.F.; Mundell, C.G. VLBA Identification of the Milliarcsecond Active Nucleus in the Seyfert Galaxy NGC 4151. *aj* **2005**, *130*, 936–944, [arXiv:astro-ph/astro-ph/0505141]. doi:10.1086/432034.
39. Harrison, B.; Pedlar, A.; Unger, S.W.; Burgess, P.; Graham, D.A.; Preuss, E. The parsec-scale structure of the radio nucleus of NGC 4151. *mnras* **1986**, *218*, 775–784. doi:10.1093/mnras/218.4.775.
40. Ulvestad, J.S.; Roy, A.L.; Colbert, E.J.M.; Wilson, A.S. A Subparsec Radio Jet or Disk in NGC 4151. *apj* **1998**, *496*, 196–202. doi:10.1086/305382.
41. Williams, D.R.A.; McHardy, I.M.; Baldi, R.D.; Beswick, R.J.; Argo, M.K.; Dullo, B.T.; Knapen, J.H.; Brinks, E.; Fenech, D.M.; Mundell, C.G.; Muxlow, T.W.B.; Panessa, F.; Rampadarath, H.; Westcott, J. Radio jets in NGC 4151: where eMERLIN meets HST. *mnras* **2017**, *472*, 3842–3853, [arXiv:astro-ph.GA/1708.07011]. doi:10.1093/mnras/stx2205.
42. Evans, I.N.; Tsvetanov, Z.; Kriss, G.A.; Ford, H.C.; Caganoff, S.; Koratkar, A.P. Hubble Space Telescope Imaging of the Narrow-Line Region of NGC 4151. *apj* **1993**, *417*, 82. doi:10.1086/173292.
43. Das, V.; Crenshaw, D.M. Mapping the Kinematics of the Narrow-Line Regions in NGC 4151 and NGC 1068. American Astronomical Society Meeting Abstracts, 2003, Vol. 203, *American Astronomical Society Meeting Abstracts*, p. 56.01.
44. Wang, J.; Fabbiano, G.; Elvis, M.; Risaliti, G.; Karovska, M.; Zezas, A.; Mundell, C.G.; Dumas, G.; Schinnerer, E. A Deep Chandra ACIS Study of NGC 4151. III. The Line Emission and Spectral Analysis of the Ionization Cone. *apj* **2011**, *742*, 23, [arXiv:astro-ph.CO/1103.1913]. doi:10.1088/0004-637X/742/1/23.
45. Goosmann, R.W.; Matt, G. Spotting the misaligned outflows in NGC 1068 using X-ray polarimetry. *mnras* **2011**, *415*, 3119–3128, [arXiv:astro-ph.HE/1012.4652]. doi:10.1111/j.1365-2966.2011.18923.x.
46. Marin, F.; Schartmann, M. Polarized radiative transfer modeling of warped and clumpy dusty tori. *aap* **2017**, *607*, A37, [arXiv:astro-ph.GA/1708.06528]. doi:10.1051/0004-6361/201731190.

Preprints.org (www.preprints.org) | NOT PEER-REVIEWED | Posted: 17 June 2024 doi:10.20944/preprints202406.1150.v1

47. Marin, F. A complete disclosure of the hidden type-1 AGN in NGC 1068 thanks to 52 yr of broad-band polarimetric observation. *mnras* **2018**, *479*, 3142–3154, [arXiv:astro-ph.GA/1806.04415]. doi:10.1093/mnras/sty1566.
48. Arévalo, P.; Bauer, F.E.; Puccetti, S.; Walton, D.J.; Koss, M.; Boggs, S.E.; Brandt, W.N.; Brightman, M.; Christensen, F.E.; Comastri, A.; Craig, W.W.; Fuerst, F.; Gandhi, P.; Grefenstette, B.W.; Hailey, C.J.; Harrison, F.A.; Luo, B.; Madejski, G.; Madsen, K.K.; Marinucci, A.; Matt, G.; Saez, C.; Stern, D.; Stuhlinger, M.; Treister, E.; Urry, C.M.; Zhang, W.W. The 2-79 keV X-Ray Spectrum of the Circinus Galaxy with NuSTAR, XMM-Newton, and Chandra: A Fully Compton-thick Active Galactic Nucleus. *apj* **2014**, *791*, 81, [arXiv:astro-ph.HE/1406.3345]. doi:10.1088/0004-637X/791/2/81.
49. Matt, G.; Fiore, F.; Perola, G.C.; Piro, L.; Fink, H.H.; Grandi, P.; Matsuoka, M.; Oliva, E.; Salvati, M. A reflection-dominated X-ray spectrum discovered by ASCA in the Circinus galaxy. *mnras* **1996**, *281*, L69–L73. doi:10.1093/mnras/281.4.L69.
50. Bianchi, S.; Matt, G.; Iwasawa, K. The circumnuclear X-ray reflectors in NGC 1068 and the Circinus galaxy. *mnras* **2001**, *322*, 669–680, [arXiv:astro-ph/astro-ph/0010485]. doi:10.1046/j.1365-8711.2001.04156.x.
51. Marinucci, A.; Miniutti, G.; Bianchi, S.; Matt, G.; Risaliti, G. A Chandra view of the clumpy reflector at the heart of the Circinus galaxy. *mnras* **2013**, *436*, 2500–2504, [arXiv:astro-ph.CO/1309.4456]. doi:10.1093/mnras/stt1759.
52. Marconi, A.; Moorwood, A.F.M.; Origlia, L.; Oliva, E. A prominent ionization cone and starburst ring in the nearby Circinus galaxy. *The Messenger* **1994**, *78*, 20–24.
53. Elmouttie, M.; Haynes, R.F.; Jones, K.L.; Sadler, E.M.; Ehle, M. Radio continuum evidence for nuclear outflow in the Circinus galaxy. *mnras* **1998**, *297*, 1202–1218. doi:10.1046/j.1365-8711.1998.01592.x.
54. Curran, S.J.; Koribalski, B.S.; Bains, I. The large-scale atomic and molecular gas in the Circinus galaxy. *mnras* **2008**, *389*, 63–74, [arXiv:astro-ph/0807.4766]. doi:10.1111/j.1365-2966.2008.13574.x.
55. Greenhill, L.J.; Booth, R.S.; Ellingsen, S.P.; Herrnstein, J.R.; Jauncey, D.L.; McCulloch, P.M.; Moran, J.M.; Norris, R.P.; Reynolds, J.E.; Tzioumis, A.K. A Warped Accretion Disk and Wide-Angle Outflow in the Inner Parsec of the Circinus Galaxy. *apj* **2003**, *590*, 162–173, [arXiv:astro-ph/astro-ph/0302533]. doi:10.1086/374862.
56. Ursini, F.; Marinucci, A.; Matt, G.; Bianchi, S.; Marin, F.; Marshall, H.L.; Middei, R.; Poutanen, J.; Rogantini, D.; De Rosa, A.; Di Gesu, L.; García, J.A.; Ingram, A.; Kim, D.E.; Krawczynski, H.; Puccetti, S.; Soffitta, P.; Svoboda, J.; Tombesi, F.; Weisskopf, M.C.; Barnouin, T.; Perri, M.; Podgorny, J.; Ratheesh, A.; Zaino, A.; Agudo, I.; Antonelli, L.A.; Bachetti, M.; Baldini, L.; Baumgartner, W.H.; Bellazzini, R.; Bongiorno, S.D.; Bonino, R.; Brez, A.; Bucciantini, N.; Capitanio, F.; Castellano, S.; Cavazzuti, E.; Ciprini, S.; Costa, E.; Del Monte, E.; Di Lalla, N.; Di Marco, A.; Donnarumma, I.; Doroshenko, V.; Dovciak, M.; Ehlert, S.R.; Enoto, T.; Evangelista, Y.; Fabiani, S.; Ferrazzoli, R.; Gunji, S.; Heyl, J.; Iwakiri, W.; Jorstad, S.G.; Karas, V.; Kitaguchi, T.; Kolodziejczak, J.J.; La Monaca, F.; Latronico, L.; Liodakis, I.; Maldera, S.; Manfreda, A.; Marscher, A.P.; Mitsuishi, I.; Mizuno, T.; Muleri, F.; Ng, C.Y.; O'Dell, S.L.; Omodei, N.; Oppedisano, C.; Papitto, A.; Pavlov, G.G.; Peirson, A.L.; Pesce-Rollins, M.; Petrucci, P.O.; Pilia, M.; Possenti, A.; Ramsey, B.D.; Rankin, J.; Romani, R.W.; Sgrò, C.; Slane, P.; Spandre, G.; Tamagawa, T.; Tavecchio, F.; Taverna, R.; Tawara, Y.; Tennant, A.F.; Thomas, N.E.; Trois, A.; Tsygankov, S.S.; Turolla, R.; Vink, J.; Wu, K.; Xie, F.; Zane, S. Mapping the circumnuclear regions of the Circinus galaxy with the Imaging X-ray Polarimetry Explorer. *mnras* **2023**, *519*, 50–58, [arXiv:astro-ph.HE/2211.01697]. doi:10.1093/mnras/stac3189.
57. Bauer, F.E.; Arévalo, P.; Walton, D.J.; Koss, M.J.; Puccetti, S.; Gandhi, P.; Stern, D.; Alexander, D.M.; Baloković, M.; Boggs, S.E.; Brandt, W.N.; Brightman, M.; Christensen, F.E.; Comastri, A.; Craig, W.W.; Del Moro, A.; Hailey, C.J.; Harrison, F.A.; Hickox, R.; Luo, B.; Markwardt, C.B.; Marinucci, A.; Matt, G.; Rigby, J.R.; Rivers, E.; Saez, C.; Treister, E.; Urry, C.M.; Zhang, W.W. NuSTAR Spectroscopy of Multi-component X-Ray Reflection from NGC 1068. *apj* **2015**, *812*, 116, [arXiv:astro-ph.HE/1411.0670]. doi:10.1088/0004-637X/812/2/116.
58. Ghisellini, G.; Haardt, F.; Matt, G. The contribution of the obscuring torus to the X-ray spectrum of Seyfert galaxies: a test for the unification model. *mnras* **1994**, *267*, 743–754, [arXiv:astro-ph/astro-ph/9401044]. doi:10.1093/mnras/267.3.743.
59. Ratheesh, A.; Matt, G.; Tombesi, F.; Soffitta, P.; Pesce-Rollins, M.; Di Marco, A. Exploring the accretion-ejection geometry of GRS 1915+105 in the obscured state with future X-ray spectro-polarimetry. *aap* **2021**, *655*, A96, [arXiv:astro-ph.HE/2109.00419]. doi:10.1051/0004-6361/202140701.

Preprints.org (www.preprints.org) | NOT PEER-REVIEWED | Posted: 17 June 2024 doi:10.20944/preprints202406.1150.v1

60. Kudoh, Y.; Wada, K.; Kawakatu, N.; Nomura, M. Multiphase Gas Nature in the Sub-parsec Region of the Active Galactic Nuclei. I. Dynamical Structures of Dusty and Dust-free Outflow. *apj* **2023**, *950*, 72, [arXiv:astro-ph.GA/2304.05950]. doi:10.3847/1538-4357/accc2b.
61. Tanimoto, A.; Wada, K.; Kudoh, Y.; Odaka, H.; Uematsu, R.; Ogawa, S. Circumnuclear Multiphase Gas in the Circinus Galaxy. V. The Origin of the X-Ray Polarization in the Circinus Galaxy. *apj* **2023**, *958*, 150, [arXiv:astro-ph.HE/2310.18396]. doi:10.3847/1538-4357/ad06ac.
62. Antonucci, R. Unified models for active galactic nuclei and quasars. *araa* **1993**, *31*, 473–521. doi:10.1146/annurev.aa.31.090193.002353.
63. Marin, F.; Marinucci, A.; Laurenti, M.; Kim, D.E.; Barnouin, T.; Di Marco, A.; Ursini, F.; Bianchi, S.; Ravi, S.; Marshall, H.L.; Matt, G.; Chen, C.T.; Gianolli, V.E.; Ingram, A.; Maksym, W.P.; Panagiotou, C.; Podgorny, J.; Puccetti, S.; Ratheesh, A.; Tombesi, F.; Agudo, I.; Antonelli, L.A.; Bachetti, M.; Baldini, L.; Baumgartner, W.; Bellazzini, R.; Bongiorno, S.; Bonino, R.; Brez, A.; Bucciantini, N.; Capitanio, F.; Castellano, S.; Cavazzuti, E.; Ciprini, S.; Costa, E.; De Rosa, A.; Del Monte, E.; Di Gesu, L.; Di Lalla, N.; Donnarumma, I.; Doroshenko, V.; Dovciak, M.; Ehlert, S.; Enoto, T.; Evangelista, Y.; Fabiani, S.; Ferrazzoli, R.; Garcia, J.; Gunji, S.; Heyl, J.; Iwakiri, W.; Jorstad, S.; Kaaret, P.; Karas, V.; Kislat, F.; Kitaguchi, T.; Kolodziejczak, J.; Krawczynski, H.; La Monaca, F.; Latronico, L.; Liodakis, I.; Madejski, G.; Maldera, S.; Manfreda, A.; Marscher, A.; Massaro, F.; Mitsuishi, I.; Mizuno, T.; Muleri, F.; Negro, M.; Ng, S.; O'Dell, S.; Omodei, N.; Oppedisano, C.; Papitto, A.; Pavlov, G.; Perri, M.; Pesce-Rollins, M.; Petrucci, P.O.; Pilia, M.; Possenti, A.; Poutanen, J.; Ramsey, B.; Rankin, J.; Roberts, O.; Romani, R.; Sgro, C.; Slane, P.; Soffitta, P.; Spandre, G.; Swartz, D.; Tamagawa, T.; Tavecchio, F.; Taverna, R.; Tawara, Y.; Tennant, A.; Thomas, N.; Trois, A.; Tsygankov, S.; Turolla, R.; Vink, J.; Weisskopf, M.; Wu, K.; Xie, F.; Zane, S. X-ray polarization measurement of the gold standard of radio-quiet active galactic nuclei : NGC 1068. *arXiv e-prints* **2024**, p. arXiv:2403.02061, [arXiv:astro-ph.HE/2403.02061]. doi:10.48550/arXiv.2403.02061.
64. Antonucci, R.; Hurt, T.; Miller, J. HST Ultraviolet Spectropolarimetry of NGC 1068. *apj* **1994**, *430*, 210. doi:10.1086/174395.
65. Krawczynski, H.; Muleri, F.; Dovčiak, M.; Veledina, A.; Rodriguez Cavero, N.; Svoboda, J.; Ingram, A.; Matt, G.; Garcia, J.A.; Loktev, V.; Negro, M.; Poutanen, J.; Kitaguchi, T.; Podgorný, J.; Rankin, J.; Zhang, W.; Berdyugin, A.; Berdyugina, S.V.; Bianchi, S.; Blinov, D.; Capitanio, F.; Di Lalla, N.; Draghis, P.; Fabiani, S.; Kagitani, M.; Kravtsov, V.; Kiehlmann, S.; Latronico, L.; Lutovinov, A.A.; Mandarakas, N.; Marin, F.; Marinucci, A.; Miller, J.M.; Mizuno, T.; Molkov, S.V.; Omodei, N.; Petrucci, P.O.; Ratheesh, A.; Sakanoi, T.; Semena, A.N.; Skalidis, R.; Soffitta, P.; Tennant, A.F.; Thalhammer, P.; Tombesi, F.; Weisskopf, M.C.; Wilms, J.; Zhang, S.; Agudo, I.; Antonelli, L.A.; Bachetti, M.; Baldini, L.; Baumgartner, W.H.; Bellazzini, R.; Bongiorno, S.D.; Bonino, R.; Brez, A.; Bucciantini, N.; Castellano, S.; Cavazzuti, E.; Ciprini, S.; Costa, E.; De Rosa, A.; Del Monte, E.; Di Gesu, L.; Di Marco, A.; Donnarumma, I.; Doroshenko, V.; Ehlert, S.R.; Enoto, T.; Evangelista, Y.; Ferrazzoli, R.; Gunji, S.; Hayashida, K.; Heyl, J.; Iwakiri, W.; Jorstad, S.G.; Karas, V.; Kolodziejczak, J.J.; La Monaca, F.; Liodakis, I.; Maldera, S.; Manfreda, A.; Marscher, A.P.; Marshall, H.L.; Mitsuishi, I.; Ng, C.Y.; O'Dell, S.L.; Oppedisano, C.; Papitto, A.; Pavlov, G.G.; Peirson, A.L.; Perri, M.; Pesce-Rollins, M.; Pilia, M.; Possenti, A.; Puccetti, S.; Ramsey, B.D.; Romani, R.W.; Sgrò, C.; Slane, P.; Spandre, G.; Tamagawa, T.; Tavecchio, F.; Taverna, R.; Tawara, Y.; Thomas, N.E.; Trois, A.; Tsygankov, S.; Turolla, R.; Vink, J.; Wu, K.; Xie, F.; Zane, S. Polarized x-rays constrain the disk-jet geometry in the black hole x-ray binary Cygnus X-1. *Science* **2022**, *378*, 650–654, [arXiv:astro-ph.HE/2206.09972]. doi:10.1126/science.add5399.
66. Stalevski, M.; Asmus, D.; Tristram, K.R.W. Dissecting the active galactic nucleus in Circinus - I. Peculiar mid-IR morphology explained by a dusty hollow cone. *mnras* **2017**, *472*, 3854–3870, [arXiv:astro-ph.GA/1708.07838]. doi:10.1093/mnras/stx2227.
67. García-Burillo, S.; Combes, F.; Ramos Almeida, C.; Usero, A.; Alonso-Herrero, A.; Hunt, L.K.; Rouan, D.; Aalto, S.; Querejeta, M.; Viti, S.; van der Werf, P.P.; Vives-Arias, H.; Fuente, A.; Colina, L.; Martín-Pintado, J.; Henkel, C.; Martín, S.; Krips, M.; Gratadour, D.; Neri, R.; Tacconi, L.J. ALMA images the many faces of the <ASTROBJ>NGC 1068</ASTROBJ> torus and its surroundings. *aap* **2019**, *632*, A61, [arXiv:astro-ph.GA/1909.00675]. doi:10.1051/0004-6361/201936606.
68. Vermot, P.; Clénet, Y.; Gratadour, D.; Rouan, D.; Grosset, L.; Perrin, G.; Kervella, P.; Paumard, T. The inner hot dust in the torus of NGC 1068. A 3D radiative model constrained with GRAVITY/VLTi. *aap* **2021**, *652*, A65, [arXiv:astro-ph.GA/2106.04211]. doi:10.1051/0004-6361/202141349.

Preprints.org (www.preprints.org) | NOT PEER-REVIEWED | Posted: 17 June 2024 doi:10.20944/preprints202406.1150.v1

Disclaimer/Publisher's Note: The statements, opinions and data contained in all publications are solely those of the individual author(s) and contributor(s) and not of MDPI and/or the editor(s). MDPI and/or the editor(s) disclaim responsibility for any injury to people or property resulting from any ideas, methods, instructions or products referred to in the content.